MOLECULAR PHARMACOLOGY, 25:92–101

The Nature of the Interactions of Pyridostigmine with the Nicotinic Acetylcholine Receptor-Ionic Channel Complex

I. Agonist, Desensitizing, and Binding Properties

GARY J. PASCUZZO,[1] AKINORI AKAIKE, MOHAMMED A. MALEQUE,[2] KAI-PING SHAW, ROBERT S. ARONSTAM,[3] DANIEL L. RICKETT,[1] AND EDSON X. ALBUQUERQUE

Department of Pharmacology and Experimental Therapeutics, University of Maryland School of Medicine, Baltimore, Maryland 21201

Received April 19, 1983; Accepted September 30, 1983

SUMMARY

The actions of pyridostigmine (Pyr), an anticholinesterase agent, were studied on the acetylcholine (ACh) receptor-ion channel complex and on the electrically excitable membrane of the frog cutaneous pectoris and sartorius muscles and the chronically denervated soleus muscle of the rat. Pyr at concentrations of 0.2–0.4 mM potentiated the indirect evoked muscle twitch and at concentrations ≥0.8 mM depressed the indirect twitch with an IC_{50} of about 2 mM. Twitch depression produced by Pyr was reversed slowly, and after a 60-min wash only 59% of the control muscle twitch had returned. Pyr did not affect either the membrane potential or the muscle action potential. Pyr had several effects at the neuromuscular junction of the frog and rat. It decreased the peak amplitude of the end-plate current (EPC) in a voltage- and concentration-dependent manner. In contrast to diisopropylfluorophosphate, which depresses the EPC amplitude and induces a double exponential decay of the EPC and miniature end-plate current (MEPC), Pyr produced a marked prolongation of the time constants of EPC and MEPC decay while maintaining a single exponential decay. The decrease caused by Pyr of indirect twitch tension, EPC amplitude, and ACh sensitivity indicates mechanisms which limit the number and/or properties of conducting channels. The drug decreased channel conductance and prolonged channel lifetime as revealed by Fourier analysis of ACh-induced end-plate current fluctuations. An altered form of the conducting species induced by Pyr appears to be responsible for either the apparent agonist-induced depolarization or its ability to increase the affinity of ACh for its recognition site. Pyr was also found to inhibit the binding of ACh and α-bungarotoxin to receptor-rich membrane from the electric organ of *Torpedo nobiliana*, and to have a higher affinity for the receptor than for the ion channel binding sites. These actions are distinct from acetylcholinesterase inhibition caused by the agent. Strong evidence suggests that the direct influences of the agent on neuromuscular transmission involve at least three distinct, although possibly interacting, mechanisms: (a) a weak agonist action, (b) the formation of desensitized receptor-complex intermediates, and (c) the alteration of the conductance properties of active channels.

INTRODUCTION

The quaternary carbamate, Pyr,[4] is a widely used medication for myasthenia gravis (1) and has also been used as a pretreatment against organophosphate agent toxicity (2). The pharmacological actions of AChE drugs are not limited to enzyme inhibition. It has long been known that other carbamates, e.g., neostigmine and physostig-

This research was supported by United States Army Medical Research and Development Command Contract DAMD17-81-C-1279.

[1] Present address, Neurotoxicology Branch, United States Army Medical Research Institute of Chemical Defense, Aberdeen Proving Ground, Aberdeen, Md. 21010.

[2] Present address, Department of Pharmacology, School of Medicine, Meharry Medical College, Nashville, Tenn. 37208.

[3] Present address, Department of Pharmacology, Medical College of Georgia, Augusta, Ga. 30912.

[4] The abbreviations used are: Pyr, pyridostigmine; AChE, acetylcholinesterase; ACh, acetylcholine; AChR, ACh receptor; DFP, diisopropylfluorophosphate; TTX, tetrodotoxin; PCP, phencyclidine; HTX, perhydrohistrionicotoxin; MEPC, miniature end-plate current; α-BGT, α-bungarotoxin; EPC, end-plate current; τ_{EPC}, decay time constant of EPC; τ_I, channel lifetime; τ_{MEPC}, decay time constant of miniature end-plate current; γ, single-channel conductance; IC_{50}, 50% inhibitory concentration.

0026-895X/84/010092-10$02.00/0

mine (eserine), have quite diverse effects on electrical events at neuromuscular junctions (3, 4). Some of these effects may be due to AChE inhibition and the resulting accumulation of ACh in the synaptic cleft (5, 6), although alternative interpretations have been presented (7, 8). In addition, some effects appear to be due to presynaptic alterations (9, 10). Yet other effects seem to reflect mechanisms involving nicotinic AChRs at the muscle membrane; the curare-like depression of ACh sensitivity in the presence of carbamates (4) may be due to competitive inhibition (11) or binding to other sites on the AChR (12). Such direct receptor interactions could affect the rate constants of ACh-induced conformational changes (8).

Because of the multiple sites for drug interaction at the neuromuscular junction, it is difficult to delineate specific mechanisms underlying any of the above-mentioned diverse effects of carbamates. The objective of this study is to identify mechanisms involved in Pyr interactions with the macromolecule comprising the nicotinic receptor ion channel complex. For this purpose we have used both biophysical and biochemical techniques. The present result demonstrates that, in addition to the well-known inhibition of AChE produced by Pyr, the agent has a direct interaction with the AChR-ion channel complex.

This paper deals with the action of Pyr on EPCs, ACh sensitivity, and EPC fluctuations caused by ACh microiontophoresis. It also describes binding studies of this agent with the nicotinic receptor of the *Torpedo nobiliana* electric organ. The companion paper (13) discusses patch clamp studies of the effects of Pyr on the single-channel events generated by activation of AChR-ion channel complex.

MATERIALS AND METHODS

Tissue preparations, solutions and drugs. All data were collected at room temperature (20–22°) from sartorius or cutaneous pectoris muscle of the frog, *Rana pipiens*, or from chronically denervated (7–14 days) soleus muscle of the Wistar rat (180–200 g). The physiological solution for the frog muscles had the following composition (millimolar): NaCl, 116; KCl, 2.0; $CaCl_2$, 1.8; Na_2HPO_4, 1.3; and NaH_2PO_4, 0.7. The frog Ringer's solution was bubbled with 100% O_2 and had a pH of 6.9–7.1. The physiological solution for mammalian muscle had the following composition (millimolar): NaCl, 135; KCl, 5.0; $MgCl_2$, 1.0; $CaCl_2$, 2.0; $NaHCO_3$, 15.0; and Na_2HPO_4, 1.0. The solution was continuously aerated with 95% O_2/5% CO_2, and the pH was 7.1–7.2.

Pyr bromide (Hoffmann-La Roche) and DFP (Sigma) were prepared fresh daily. TTX was also freshly prepared from stock solutions of 3×10^{-4} M. For MEPC and ACh-iontophoresis experiments, 0.3 μM tetrodotoxin was included in all solutions.

Electrophysiological techniques. Twitch studies were performed on frog sartorius muscle with sciatic nerve attached. Direct muscle stimulation was applied by a platinum bipolar electrode using supramaximal square-wave pulses of 2–3 msec duration. Indirect stimulation was applied via the sciatic nerve by a separate platinum bipolar electrode using supramaximal square-wave pulses of 0.05–0.1 msec duration. Indirect stimulation volleys were applied at a frequency of 0.2 Hz. To study direct evoked muscle twitch, neuromuscular transmission was blocked α-BGT (5 μg/ml). In all experiments the sartorius muscle was allowed to equilibrate in the stimulation conditions for 20–30 min before addition of drug. For each drug concentration, the time of exposure was chosen to allow for maximal effects to be observed; the exposures ranged from 15 to 45 min with maximal effects usually occurring 10–20 min after the addition of a new drug concentration.

Intracellular electrodes were filled with 3 M KCl and had resistances of 1–4 Mohm. Action potentials were evoked directly by passing a 30-msec depolarizing pulse through one microelectrode inserted into a surface fiber about 50 μm from the recording electrode. The action potential with its rate of rise and fall, measured via an RC circuit (1 Mohm–100 pF), was displayed on an oscilloscope and photographed.

EPC analysis. Frog sartorius muscles with nerve attached were treated with 400–600 mM glycerol to disrupt excitation-contraction coupling. The voltage-clamp circuit was similar to that of Takeuchi and Takeuchi (14) as modified by Kuba *et al.* (7). The membrane voltage sequence for EPC experiments consisted of 10-mV conditioning steps made in both depolarizing and hyperpolarizing directions throughout the range of +60 to −160 mV. Occasionally, larger steps were used in order to check for hysteresis (for details see ref. 15). Each conditioning step was 3 sec in duration; at the end of each conditioning step an EPC was elicited by nerve stimulation. This 3-sec duration sequence avoided the noticeable frequency-dependent effects of Pyr. The EPC waveforms were displayed on an oscilloscope and digitized at 10 KHz by a PDP 11/40 minicomputer (Digital Equipment Corporation). The rise times and peak amplitudes were obtained directly from the digitized EPC data. The decay phase (80%–20%) was fit by a single exponential (linear regression on the logarithms of the data points) from which the EPC decay time constant (τ_{EPC}) was determined.

MEPC and EPC fluctuation (noise) analysis. For the spontaneous MEPC and EPC fluctuation experiments, the signals were sampled at the junctional region of surface fibers of the cutaneous pectoris muscles, using conventional techniques for recording and analysis (15–17). Unfiltered signals were recorded on an FM tape recorder (Racal 4DS) and displayed on a Mingograf 81 chart recorder (frequency response dc–700 Hz). MEPCs were filtered (1–2500 Hz) by a bandpass filter (Krohn-Hite 3700) and briefly stored in a digital oscilloscope (Gould OS4000) before being transmitted to the PDP 11/40 computer for signal averaging and analysis. The ACh-induced noise was displayed as a low-gain dc trace on the Mingograf for mean current measurement and at high-gain on the FM tape recorder for current fluctuation measurement. The high-gain noise signal was filtered from 1 to 800 Hz and digitized at 2 KHz. After records containing either MEPCs or electrical artifacts were removed, a Fourier analysis was performed on 512-point samples. Each spectrum is the difference between the average of about 30 baseline and 30 ACh spectra. The power density spectrum of the noise was fit to a single Lorentzian function using a nonlinear regression program. The single-channel lifetime (τ_I) was obtained from the half-power frequency (f_c) of the Lorentzian curve ($\tau_I = 1/2\pi f_c$). The single-channel conductance (γ) was calculated using the expression $\gamma = S(0)/4\mu(V_m - V_{eq})\tau_I$, where μ is the mean dc current, V_m is the holding potential, $V_{eq} = -15$ mV is the equilibrium potential, and $S(0)$ is the zero-frequency asymptote.

Double-barrel ACh microiontophoresis. The details of this technique have been described previously (18). Both barrels of a double-barrel microiontophoretic pipette were filled with 2 M ACh. One barrel of the micropipette was used for microiontophoresis of a long (30 sec) conditioning charge to release ACh, while the other barrel was used to deliver repetitive (1 Hz), brief (50–100 μsec) charges. The position of the double-barrel micropipette was adjusted so that the 50-μsec charges applied to the ACh pipette induced a response of <1.0 msec rise time. A single intracellular microelectrode measured the transient membrane depolarizations due to ACh. The decrease of ACh potential amplitudes delivered at 1 Hz during the conditioning pulse and the recovery time of the amplitudes after the end of the conditioning pulse are measures of desensitization.

Binding studies. Torpedo nobiliana electric organs were purchased from Biofish Associated (Georgetown, Mass.) and stored at −70° for up to 2 months before use. *T. nobiliana* electrocytes bound nicotinic receptor and ion channel probes in essentially the same manner as those from *T. ocellata* (19). Electrocyte membranes were prepared by homogenization for 30 sec in 5 volumes of 50 mM Tris-HCl (pH 7.4) in

a Waring blender set at the highest speed. After filtering through four layers of cheesecloth, the suspension was centrifuged at 15,000 × *g* for 20 min. The pellets were resuspended in fresh buffer and used without further treatment. Protein content was determined by a modification of the method of Lowry *et al.* (20).

Ion channel binding was measured using two tritiated probes: PCP (piperidyl-3,4-^{3}H(*N*)-PCP, 48 Ci/mmole, New England Nuclear Corporation) and HTX ([^{3}H]H_{12}-HTX, 54.5 Ci/mmole, custom-prepared [by reduction of octahydrohistrionicotoxin with tritium gas] by New England Nuclear Corporation for Dr. J. W. Daly, of the National Institutes of Health). For further details see refs. 21 and 22.

Nicotinic receptor binding was measured using [^{125}I]α-BGT (New England Nuclear Corporation) and [^{3}H]ACh. *Torpedo* membranes (10–15 μg of protein) were incubated with the appropriate ligands (i.e., Pyr or carbamylcholine) for 20 min in Tris-HCl (pH 7.4) before initiation of the binding reaction by addition of 5 nM [^{125}I]α-BGT (incubation volume = 1 ml). After 20 min, the reaction was quenched by addition of 0.5 ml of 10 mg/ml bovine serum albumin (Sigma) which had been methylated by the method of Mandell and Hershey (23). The suspensions were then filtered through Whatman GF/B filters which had been soaked in the albumin solution to reduce binding to the filters. The radioactivity content of the filters were determined by *gamma* scintillation counting. [^{3}H]ACh (80 Ci/mmole, prepared by acetylation of [^{3}H]choline purchased from New England Nuclear Corporation and generously provided by Dr. J. J. Buccafusco) binding was measured by equilibrium dialysis. An aliquot of suspended *Torpedo* electric organ membranes was placed inside cellulose tubing (Spectra/Por 2, Fisher Scientific Company) and the tube was sealed at both ends and placed in a 20-ml bath containing 10 nM [^{3}H]ACh and 100 mM Tris-HCl (pH 7.4). After incubating for 4 hr at room temperature on a rotary shaker, 50-μl aliquots were taken from the bath sealed tubes and analyzed for radioactivity content by liquid scintillation counting. The tissue was pretreated with 100 μM DFP (Sigma Chemical Company) for 30 min at room temperature to inhibit AChE. Nonspecific binding was determined by including 100 μM nicotine in a parallel series of incubation media.

Statistics. Where applicable, data are expressed as means ± standard error of the mean. The two-tailed Student's *t*-test was used for statistical comparisons. Values of $p < 0.05$ were considered as statistically significant.

RESULTS

Effects of Pyr on muscle twitch tension, membrane resting potential, and action potential. The concentration-dependent effect of Pyr (0.1–4.8 mM) on the indirect twitch tension of the frog sartorius muscle is shown in Fig. 1. At concentrations of 0.2–0.4 mM there was a marked potentiation (117–140% of control) of the indirect twitch. At concentrations ≥0.8 mM the indirect muscle twitch was depressed in a concentration-dependent manner with complete blockade to <5% of control occurring at 4.8 mM. The 50% inhibitory concentration (IC_{50}) for depression of indirect twitch was about 2 mM Pyr. Following the application of 4.8 mM Pyr for 30 min and subsequent repetitive washing for 1 hr, the indirect twitch remained depressed to 59% of control amplitude. When α-BGT (5 μg/ml) was used to inhibit the indirect twitch completely, Pyr (4.8 mM) was found to have no effect on the direct twitch.

Extrajunctional recordings (2–5 mm away from the junctional area) of resting membrane potential along the surface fibers of the cutaneous pectoris revealed no effects of Pyr at concentrations up to 1 mM (−91.6 ± 1.1 mV, $n = 30$, as opposed to control mean value −93.4 ± 1.5 mV, $n = 25$). No significant effect was observed on the threshold, amplitude, rate of rise, or half-decay time

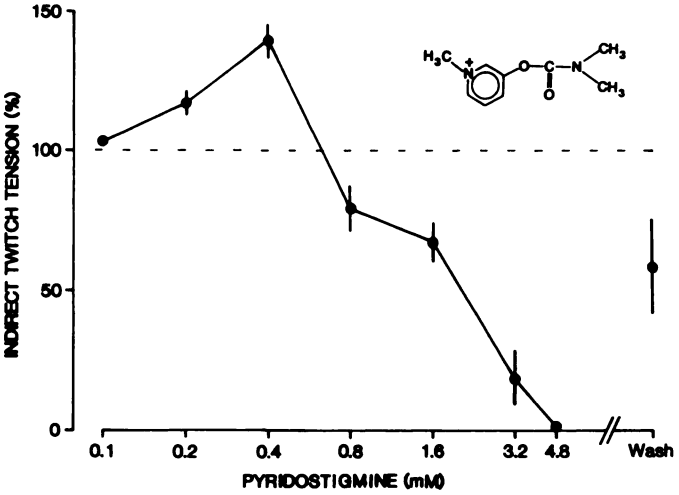

FIG. 1. *Dose-response relationship of the effect of Pyr on indirect twitch tension of frog sartorius muscle*

Twitch tension is given as percentage of the control value before the addition of drug; the data points are the mean ± standard deviation of six muscle preparations at each concentration, and the $IC_{50} \simeq 2$ mM; where no bar appears, the values are too small to be shown. After the application of 4.8 mM Pyr, each preparation was washed repetitively. (One complete change of physiological solution occurred every 10 min; bath volume, 20 ml) *Wash* indicates the amount of recovery (~50%) at 60 min. The frequency of indirectly evoked twitch was 0.2 Hz. The *inset* shows the structure of Pyr.

of directly elicited action potential recorded at junctional and extrajunctional regions.

Effects of Pyr on stimulation-evoked EPCs. Figure 2 shows the control values of EPC peak amplitude, and τ_{EPC} recorded at several voltage-clamped membrane potentials and at Pyr concentrations ranging from 10 μM to 1 mM. In comparison to control, 10 μM Pyr increased the peak amplitude of the EPC and τ_{EPC}, whereas at concentrations ≥100 μM the peak amplitude at potentials of −70 to −160 mV and τ_{EPC} at all membrane potentials were different from control (Fig. 2). Figure 2A shows the current-voltage relationship of the EPC peak amplitude at membrane potentials from −160 to +60 mV during the Pyr applications. Even at concentrations ≥100 μM, Pyr depressed the EPC peak amplitude and produced nonlinearities of the current-voltage relationship in the third quadrant. In comparison to control, at concentrations <100 μM, Pyr significantly increased the amplitude of the EPC at all membrane potentials recorded (−160 mV to +60 mV).

The data in Fig. 2 were collected at a stimulus frequency of 0.3 Hz (3-sec conditioning step; the nerve was stimulated to generate an EPC during the last 100 msec of the conditioning pulse). At this stimulus frequency, no time-dependent or hysteresis effects were observed. However, in the presence of Pyr at concentrations of ≥100 μM and at stimulus frequencies ≥1 Hz, there was a noticeable stimulation-dependent decrease in EPC peak amplitudes.

Figure 2B shows that τ_{EPC} maintained its voltage dependence while becoming greatly prolonged by Pyr at concentrations varying from 100 μM to 1 mM. It should be mentioned, however, that Pyr at 1 mM produced a slight depression of τ_{EPC} when compared with that induced by 100 μM drug, thus suggesting an effect of the

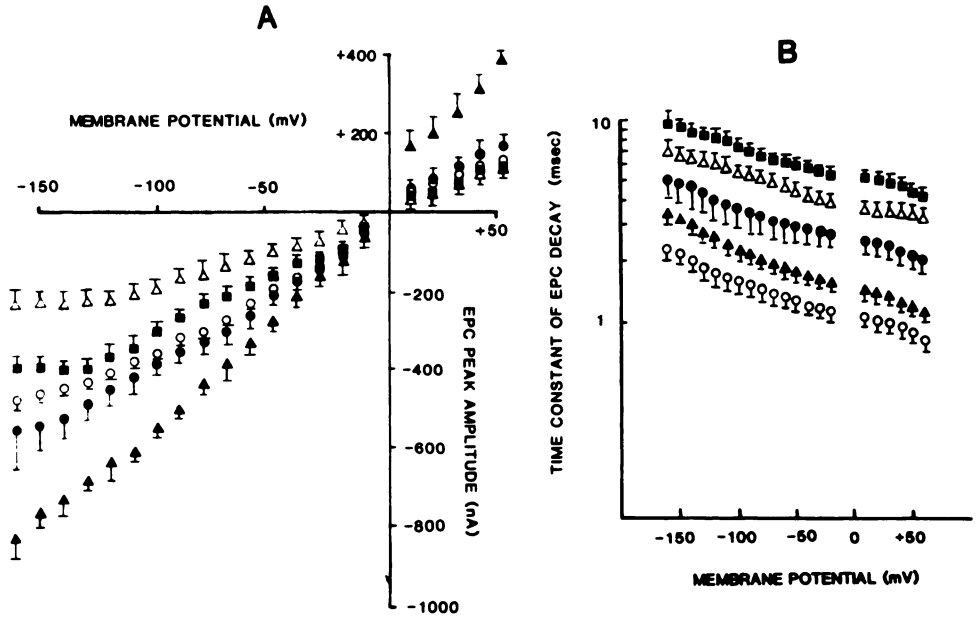

FIG. 2. *Effects of Pyr on EPC peak amplitude (A) and time constant of EPC decay (B)*
In A is shown the relationship between peak amplitude of the EPC and the membrane potential for control (○); in the presence of the Pyr concentrations, 10 μM (▲), 100 μM (■), and 1 mM (△); and after a 60-min wash (●). Each point represents the mean ± standard error of the mean of 8 to 45 surface fibers from at least 4 muscles. In B, the relationship between the logarithm of time constant of EPC decay and membrane potential under control conditions and in the presence of Pyr is shown. Symbols are the same as in A.

drug on the ACh receptor ion-channels. The prolongation of τ_{EPC} by a drug which decreases EPC amplitude is in distinct contrast to the generally decreased τ_{EPC} and/or loss of voltage sensitivity reported for the drugs atropine (24), amantadine (25), and tetraethylammonium (17). Futhermore, in contrast to scopolamine (24) and to DFP (7), the EPC decay remained a single exponential function of time for all Pyr concentrations sampled (see Fig. 3).

Effects of Pyr on the MEPCs. The concentration-dependent effects of Pyr (1 μM–1 mM) on the voltage sensitivity of the MEPC peak amplitude and τ_{MEPC} are shown in Fig. 4 and Table 1. The peak amplitude of spontaneously occurring MEPCs decreased to a lesser extent at equivalent drug concentrations and periods of incubation than that observed for EPCs. The peak amplitude of the MEPC was altered in the following manner (see Fig. 4A): no effect at 1 μM, increased at 10 μM (at −90 mV they were 122% of control), decreased at 100 μM (−90 mV, 89%), and markedly depressed by 1 mM Pyr (−90 mV, 55% control). At 10 μM the decay phase of MEPCs recorded at −60 to −120 mV remained a single exponential function of time and retained voltage sensitivity despite the significant lengthening of τ_{MEPC} (Fig. 4B).

For further comparisons, MEPC recordings in the presence of DFP and Pyr are presented in Fig. 4C. During exposure to DFP (30–45 min) and its washout, the MEPCs underwent changes similar to those described for EPCs in frog sartorius muscles (7). The peak amplitude of the MEPC decreased to 75% of control and the decay phase became double-exponential in the presence of DFP; both peak amplitude and τ_{MEPC} then increased during washout to 130% and 200% of control values, respectively. After the removal of excess DFP, the MEPC waveform represents the condition of complete AChE inhibition (7); i.e., there was an increase in the peak amplitude and marked prolongation of the decay time constant of spontaneous MEPC recorded at −100 mV (Fig. 4C, *3*). The subsequent application of 1 mM Pyr again decreased the amplitude, but the τ_{MEPC} was prolonged.

Effect of Pyr on ACh sensitivity of junctional and extrajunctional receptors. Double-barrel microiontophoretic techniques were used to apply ACh at the neuro-

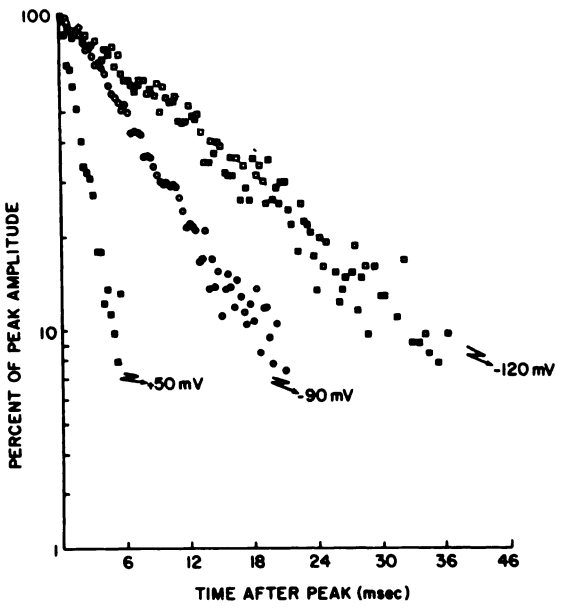

FIG. 3. *Single-exponential decay of EPC in the presence of 1 mM Pyr*
Logarithm of percentage of EPC peak amplitude versus time after the peak for three different membrane potentials.

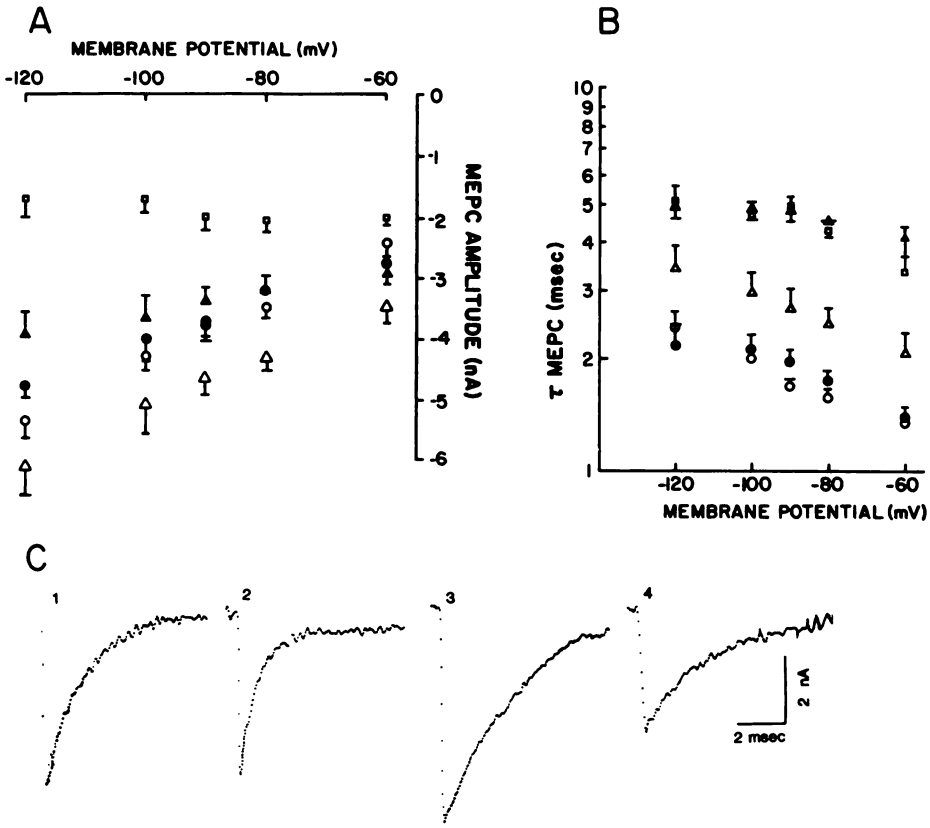

FIG. 4. *Effects of Pyr on MEPC peak amplitude and τ_{MEPC} and comparison to DFP*

In A, the relationship between peak amplitude of the MEPC and the membrane potential is shown for control conditions (O) and in the presence of Pyr, 1 μM (●), 10 μM (△), 100 μM (▲), and 1 mM (□). In B, the relationship between log (τ_{MEPC}) and the membrane potential shown for control and in the presence of Pyr; symbols are same as in A. C, Comparison of signal-averaged MEPCs recorded at −100 mV under control conditions (*1*), in the presence of 1 mM DFP (*2*), after a 2-hr washout of DFP (*3*), and after subsequent application of 1 mM Pyr (*4*). The τ_{MEPC} for control (*1*) was 2.41 msec, during DFP, τ_{fast} = 0.85 msec; τ_{slow} = 13.5 msec; after washing DFP for 60 min, τ = 4.09 msec and during Pyr, τ = 5.12 msec. The records in C were obtained from the same end-plate region.

muscular junction of the frog sartorius muscle. One barrel released ACh upon application of current with a 50-μsec duration at a frequency of 1 Hz so as to mimic MEPPs. The rise time of the brief ACh transients was usually shorter than 1 msec. The control values for ACh sensitivity at junctional region was 2670 ± 320 mV/nC. The other barrel provided a steady 30-sec ACh pulse. The decrease in the amplitude of the ACh transients during the 30-sec steady pulse has been described as a phase of desensitization, and the increase in the amplitudes 30 sec after the end of the steady pulse as the recovery phase (18, 26). In comparison to control conditions, after 30–40 min of exposure to 1 mM Pyr the amplitude of the brief ACh potentials were depressed by Pyr during the steady pulse (Fig. 5). For example, during the steady ACh pulse, the amplitude of the brief ACh transient observed under control conditions decreased to 57%, while in the presence of 1 mM Pyr it decreased to 12% of control. After 30 sec of recovery, the control was 95% as compared with 43% for 1 mM Pyr.

TABLE 1

Concentration-dependent action of Pyr on the spontaneously occurring MEPC recorded at −90 mV

Data, obtained from at least three cutaneous pectoris muscles, are the means ± standard error.

Condition	Amplitude	Rise time	τ
	namp	*msec*	*msec*
Control	3.82 ± 0.26	0.475 ± 0.012	1.63 ± 0.09
Pyr			
1 μM	3.58 ± 0.26	0.573 ± 0.017	1.87 ± 0.18
10 μM	4.38 ± 0.28	0.595 ± 0.026	2.49 ± 0.24[a]
100 μM	3.99 ± 0.68	0.604 ± 0.021	4.78 ± 0.21[a]
1 mM	2.01 ± 0.18[a]	0.656 ± 0.019[a]	4.82 ± 0.58[a]
Washout (1 hr)	3.87 ± 0.42	0.527 ± 0.042	3.23 ± 0.25

[a] $p < 0.01$.

To examine the desensitizing effects of Pyr under conditions of negligible AChE activity, similar double-barrel experiments were performed on chronically (7–10 day) denervated rat soleus muscle (18). In the presence of Pyr (Fig. 6) there was rapid desensitization during the steady pulse and a very lengthened recovery time. These effects were clearly discerned at 1 mM Pyr and became much more prononced at higher concentrations. However, another phenomenon which was present was a small ACh-induced steady membrane depolarization. This was evident before and after the long ACh pulse of 30 sec. At high concentrations (≥1 mM) both the short and long ACh transients were depressed. During the washout of 1–5 mM Pyr, control values were observed at about 2.5 hr. It should be noted that the level of desensitization observed in the innervated junctional region

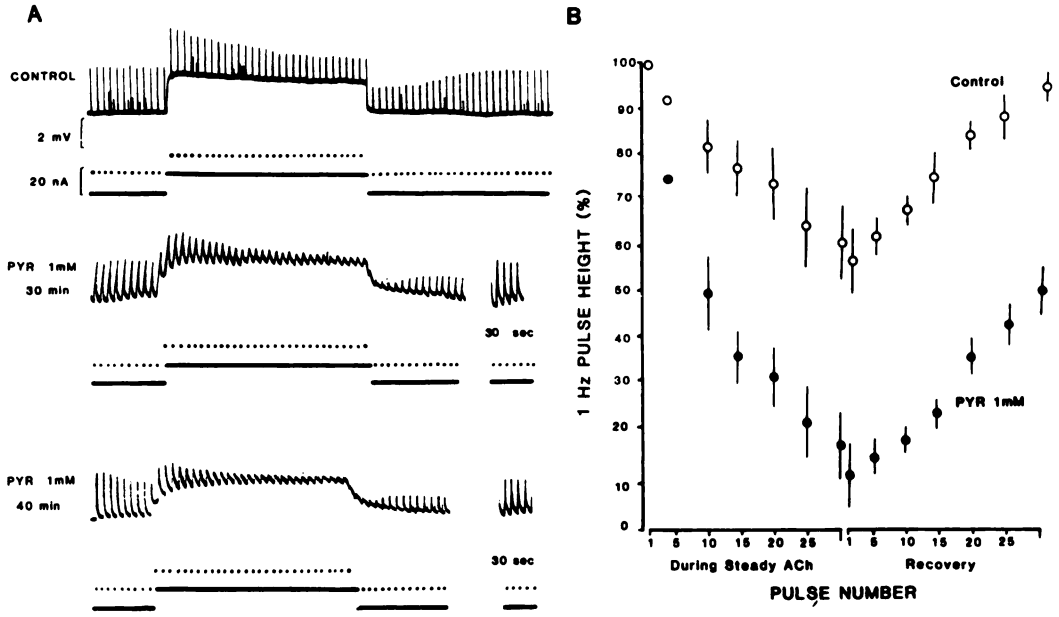

FIG. 5. *Desensitization and recovery of the nicotinic receptor-ion channel complex from the junctional region of the frog cutaneous pectoris*
In A, typical records of ACh-induced transient depolarizations due to microiontophoretic pulses of 50-μsec duration (····, retouched for clarity), 1 Hz are shown together with 30-sec conditoning pulses which released ACh (——). The top record is control, the lower two records are in the presence of 1 mM Pyr at the times indicated. In B, control and 1 mM Pyr, 40-min changes in 1-Hz pulse height are shown during and after the steady conditioning pulse expressed as percentage of average height before the conditioning pulse. Data points represent means of five determinations; standard deviation bars are indicated for the points.

was more intensive using the same concentration of Pyr than in the chronically denervated extrajunctional region. This difference may be related to the blockade of cholinesterase by Pyr at the junctional region which may cause a relatively high amount of the transmitter at the region, thus adding to the effect of the iontophoretically applied ACh.

Effects on the ionic channel of the nicotinic AChR. ACh-induced EPC fluctuations (noise) were recorded in the presence of Pyr. Figure 7 shows a typical power density spectrum obtained at a membrane potential of −85 mV with a cutoff frequency (f_c) which was shifted by Pyr (1 mM), thus disclosing a longer τ_I (139% of control) coupled with a decrease of γ by 36% of control. The noise analysis parameters γ and τ_I are presented in Table 2. These data reveal a concentration-dependent action of Pyr on the ionic channel of the nicotinic receptor. Usually, Pyr at concentrations higher than 100 μM significantly decreased γ while simultaneously increasing τ_I. When these effects of Pyr were compared with an irreversible blocker of AChE such as DFP, a marked contrast was observed. For example, during exposure to DFP, a typical double-exponential decay of the MEPC and double-Lorentzian ACh noise spectra were observed (Fig. 8). Subsequently, washout of DFP and then application of 1 mM Pyr resulted in prolongation of τ_I. As can be seen in Table 3, γ was decreased in the presence of 1 mM DFP, but, during the washout, both γ and τ_I returned to control values and τ_I came back to a single component. Consistent with previous observations, τ_I is specific for the agonist ACh (27, 28) and did not change with increasing agonist concentration alone, i.e., for the complete AChE inhibition during the washout. Yet further addition of 1 mM Pyr decreased γ and increased τ_I. Thus, Pyr is capable of antagonizing some of the effects of DFP by exerting a direct influence on the AChR ion channel complex.

Binding of Pyr to the ACh receptor. At concentrations >100 μM, Pyr inhibited the binding of both [^{3}H]ACh and [^{125}I]α-BGT to the nicotinic receptor (Fig. 9). The IC_{50} value for inhibition of receptor binding was substantially lower using [^{3}H]ACh (0.35 mM) as compared with [^{125}I]α-BGT (2.8 mM). This is not unexpected insofar as the assay conditions used, and in particular the high concentration (5 nM) of [^{125}I]α-BGT used in relation to its true dissociation constant would be expected to shift competition curves to the right. Pyr inhibition of 10 nM [^{3}H]ACh binding is probably a more accurate reflection of its affinity for the ACh receptor.

The ability of carbamylcholine to inhibit [^{125}I]α-BGT binding to the receptor was enhanced in the presence of Pyr (Fig. 10). The IC_{50} for binding inhibition decreased in a concentration-dependent fashion from 3.2 to about 0.5 μM in the presence of 1 or 3 mM Pyr. At these Pyr concentrations the level of [^{125}I]α-BGT was reduced by 30–60%.

Interaction of Pyr with the ion channel component of the ACh receptor. The influence of Pyr on [^{3}H]PCP and [^{3}H]H_{12}-HTX binding to the ion channel associated with the nicotinic ACh receptor in *Torpedo* electric organ was determined in the presence and absence of 1 μM carbamylcholine (Fig. 11). Significant stimulation was seen at Pyr concentrations as low as 30 μM. In the absence of carbamylcholine, Pyr elevated amantadine-sensitive [^{3}H]PCP binding by up to 2.5-fold at concentrations between 0.2 and 3 mM (Fig. 11). The level of this stimulation was depressed to below control levels at Pyr concentrations above 10 mM. In the presence of 1 μM car-

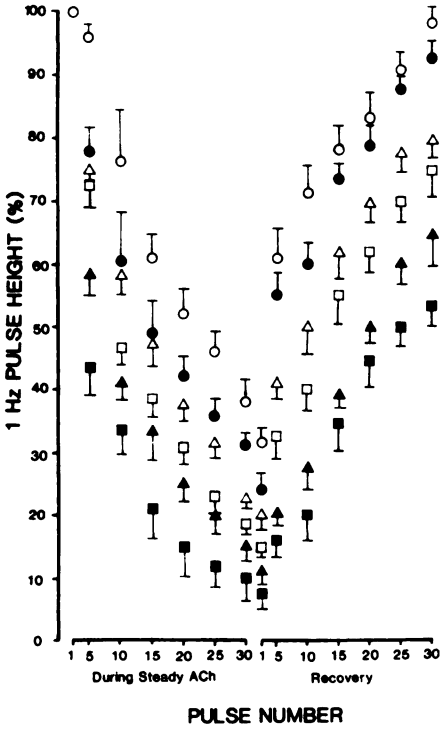

FIG. 6. *Desensitization and recovery of the nicotinic receptor-ion channel complex of the chronically denervated rat soleus muscle induced by Pyr*

Typical records obtained in a manner similar to those shown in Fig. 5. Microiontophoretic pulse to release ACh was at 1 Hz, 100-μsec duration, with 30-sec conditioning pulse. The changes in 1-Hz pulse height are shown during the steady conditioning pulse and during the recovery, expressed as percentage of average height before the conditioning pulse. Data points represent means of five determinations; standard deviation bars are indicated. The Pyr concentrations are indicated: ○, control; ●, 100 μM; △, 1 mM; □, 2 mM; ▲, 4 mM; ■, 5 mM. Note that 1 mM Pyr markedly depressed the depolarization induced by short iontophoretic pulse (50-μsec) applied to the ACh pipette.

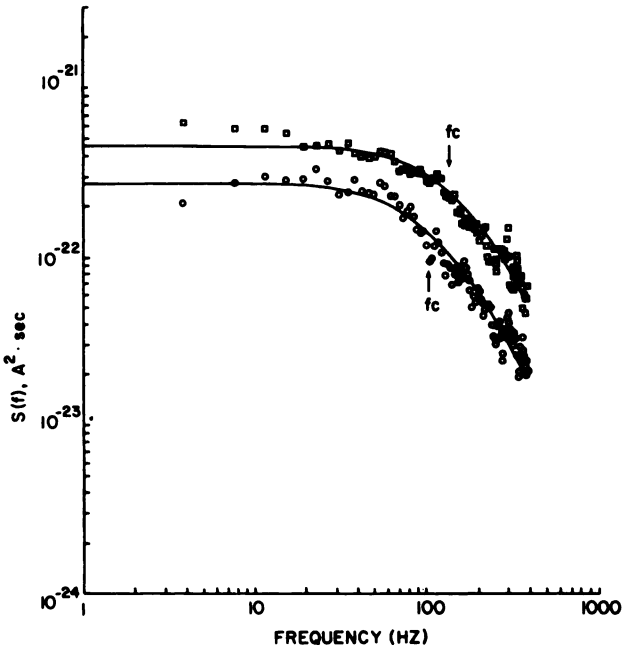

FIG. 7. *Effect of Pyr on ACh-induced EPC at the junctional region of surface fibers of the cutaneous pectoris muscle*

The power spectra of the ACh-induced EPC fluctuations obtained in the absence (□) and presence (○) of Pyr (1 mM). The lines are the best fit of the points of a single Lorentzian line using a nonlinear regression program based on the Marquardt-Levenberg algorithm. The half-power frequency (*fc*) is indicated by the *arrows* and was 143 Hz for control and 107 Hz in the presence of Pyr. Single-channel conductance and lifetime were 25.7 pS and 1.11 msec for control and 12.6 pS and 1.49 msec in the presence of the drug. The holding membrane potential was −85 mV and the temperature was 22°. The bandwidth of the filter was set to 1–800 Hz.

bamylcholine, specific 3 nM [^{3}H]PCP binding was increased 3- to 4-fold. Under these conditions, Pyr did not stimulate [^{3}H]PCP binding, and inhibited its binding at concentrations above 1 mM.

A similar pattern was obtained using [^{3}H]H_{12}-HTX as the channel probe (Fig. 11). In the absence of carbamylcholine, Pyr elevated [^{3}H]H_{12}-HTX binding by up to 50% between 0.2 and 3 mM. At concentrations above 1 mM this increase was moderated, and inhibition of binding was seen at Pyr concentrations above 10 mM. In the presence of 2 μM carbamylcholine, 2 nM [^{3}H]H_{12}-HTX binding was increased by 20%; Pyr further increased [^{3}H]H_{12}-HTX binding by as much as 33% at concentrations between 0.03 and 3 mM. At higher concentrations, [^{3}H]H_{12}-HTX binding was inhibited.

DISCUSSION

The present study shows that the anti-AChE agent Pyr has several direct effects on the nicotinic AChR of the frog and rat. The agent blocked the indirectly elicited muscle twitch, an effect which was slowly reversible and unrelated to an action on the excitable membrane. The slow reversibility of Pyr probably is related to the trapping of the compound in the lipid phase of the membrane in spite of the agent's being a quaternary compound [more fully discussed in the following paper (13)]. Pyr decreased the peak amplitude of the EPC in a voltage- and concentration-dependent manner. The agent caused a significant departure from linearity in the current-voltage relationship of the EPC at very negative membrane potentials, an effect that strongly suggests an action at the AChR-ionic channel complex which appears to be independent of AChE inhibition. These actions of

TABLE 2

Effect of Pyr on single-channel conductance (γ) and channel lifetime (τ_I) at the junctional regions of the cutaneous pectoris muscle of frog

The holding membrane potential at the junctional region of surface fibers was −75 mV and the temperature was 22°. The value *n* = number of muscles.

Concentration	*n*	γ	τ
		pS	*msec*
Control	12	26.4 ± 2.8	1.09 ± 0.07
Pyr			
100 μM	4	17.7 ± 2.2[a]	1.48 ± 0.11[b]
1 mM	8	11.7 ± 0.5[c]	1.51 ± 0.06[c]
2 mM	4	6.1 ± 0.2[c]	1.60 ± 0.15[c]

[a] $p < 0.05$.
[b] $p < 0.02$.
[c] $p < 0.01$.

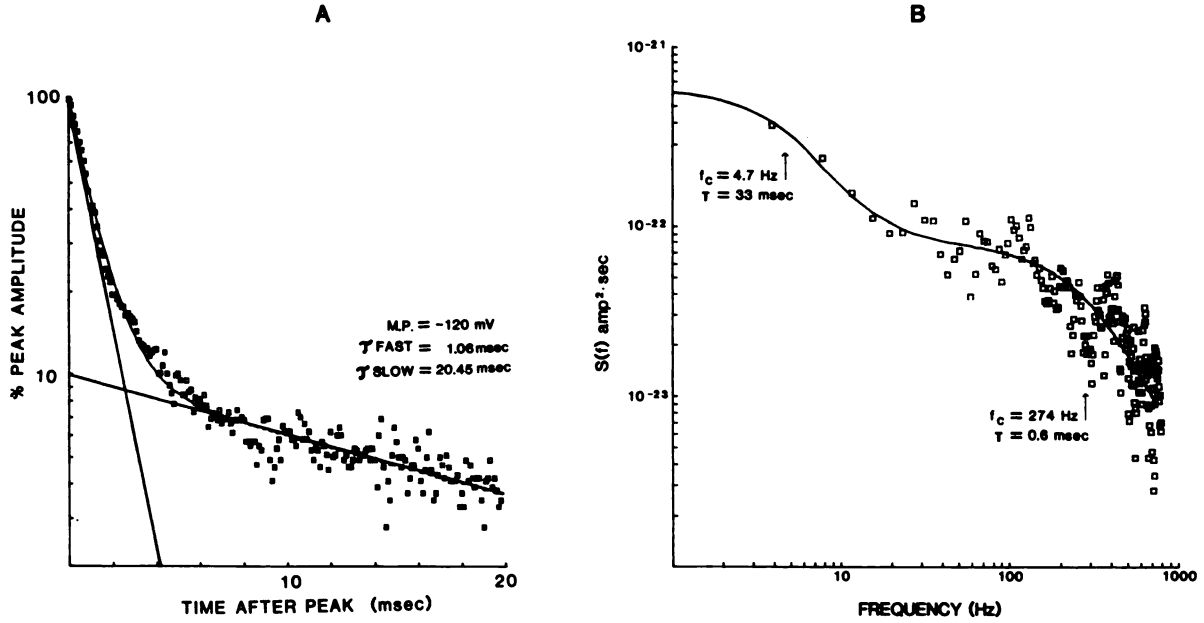

FIG. 8. *Effect of DFP on the decay phase of the end-plate current EPC (A) and on the ACh-induced EPC fluctuations (B) at the junctional region of surface fibers of the cutaneous pectoris muscle*

The EPC (A) in the presence of DFP (1 mM, 30-min exposure) was obtained from a single cell and was sent on-line to the computer and digitized at 10 KHz. The decay phase was plotted as percent of peak amplitude versus time on a semilogarithmic scale. The two components of the decay phase were fitted by the equation: $I(t) = Ae^{-T/\tau_1} + (100 - A)e^{-T/\tau_1}$, where $I(T)$ is the current (as percentage of peak amplitude) at time, t; τ_1 and τ_2 are time constants of the fast and slow components, respectively; and A is the contribution of the fast decay to the total current. A nonlinear regression program based on the Marquardt-Levenberg algorithm was used [for both EPC (A) and spectra (B)] to determine the best fit and resolve the two components. *Solid lines* of the EPC (A) represent computer-generated best fit and resolution of fast and slow components. The power spectra of the ACh-induced EPC fluctuations obtained in presence of DFP (B) also shows a double Lorentzian function. These two components of the Lorentzian function were fitted by the equation,

$$S(f) = S(0)_1 \cdot [1 + (2\pi f_c \tau_1)^2]^{-1} + S(0)_2 \cdot [1 + (2\pi f_c \tau_2)^2]^{-1}$$

The half-power frequency (f_c) is indicated by *arrows*, and the numerical values are shown in the figure. The holding membrane potential for A was −120 mV and for B was −90 mV. Temperature was 22°.

Pyr on the peak amplitude of the EPC resemble those seen with DFP (7), but, in contrast to DFP (Fig. 8), the markedly prolonged EPC and MEPC decay phases remained single-exponential in form and the decay time constant remained voltage-dependent (see Figs. 3 and 4). Pyr decreased the response of chronically denervated muscle to ACh. The decreases seen in the indirect twitch tension, the EPC amplitude, and the ACh sensitivity in the presence of Pyr indicate mechanisms which limit the number and/or properties of conducting channels. While presynaptic effects might explain some of the actions of Pyr (10, 29, 30), the decreased response to microiontophoretically applied ACh at the extrajunctional region of

TABLE 3

Reaction of Pyr with the ion channel of the nicotinic receptor after complete blockade of AChE by DFP

The control and drug effects on the single elementary phenomenon was sampled at a holding membrane potential of −75 mV. I = fast component of double-Lorentzian plot; II = slow component of double-Lorentzian plot.

	n	γ	τ
		pS	*msec*
Control	15	21.7 ± 3.8	1.01 ± 0.02
DFP, 1 mM (1 hr)	5	—[a]	I = 0.65 ± 0.03[b]
			II = 31.0 ± 4.70
Wash (2 hr)	5	26.0 ± 4.1	0.98 ± 0.03
Pyr, 1 mM (0.5 hr)	6	15.2 ± 3.6[c]	1.47 ± 0.05[c]

[a] Not evaluated.
[b] $p < 0.05$, fast component with respect to control.
[c] $p < 0.01$, with respect to wash after DFP.

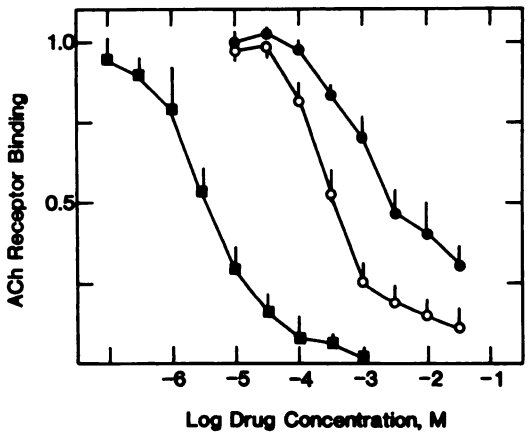

FIG. 9. *Pyr inhibition of [³H]ACh and [¹²⁵I]BGT binding to Torpedo nobiliana electrocytes*

[³H]ACh (10 nM, ○) and [¹²⁵I]α-BGT (5 nM, ●) binding, expressed as the fraction of total specific binding, was measured in the presence of the indicated Pyr concentrations. Carbamylcholine inhibition of [¹²⁵I]BGT binding (■) is included for comparison. The points and lines represent the means and standard deviations from four determinations.

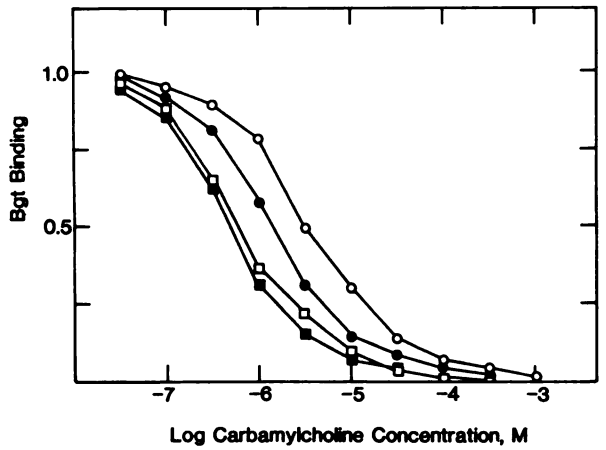

FIG. 10. *Pyr potentiation of carbamylcholine inhibition of [^{125}I]BGT binding to the nicotinic receptor*

[^{125}I]α-BGT (5 nM) binding was measured with the indicated concentrations of carbamylcholine in the presence of 1 (●), 3 (□), or 10 (■) mM Pyr, or in the absence of Pyr (○). Binding is expressed as fraction of control specific binding measured in the absence of carbamylcholine: control binding levels were decreased by 30, 53, and 60% in the presence of 1, 3, and 10 mM Pyr, respectively. Each point represents the mean from three experiments.

the denervated muscle and the nonlinearities observed in the EPC current-voltage relationships are most likely due to interactions at the postsynaptic junctional receptors.

Blockade of AChR (4, 8, 11), production of nonconducting intermediates (22), and changes in the conductance properties of the activated channels are possible modes of action, all of which may occur simultaneously in the presence of this drug.

The influence of Pyr on the binding of receptor and ion channel probes to *Torpedo nobiliana* electric organ indicates multiple interaction with the receptor-channel complex. At concentrations above 30 μM, Pyr interacts with the nicotinic receptor (i.e., the ACh binding site), inhibiting the binding of [^{3}H]ACh and [^{125}I]α-BGT and stimulating the binding of two channel probes, [^{3}H]PCP and [^{3}H]H_{12}-HTX. The nature and extent of this stimulation is consistent with that produced by other receptor ligands (19, 21). At higher concentrations, Pyr interacts with sites associated with ion translocation mechanism. This second interaction has two consequences: the binding of two known ion channel blockers ([^{3}H]PCP and [^{3}H]H_{12}-HTX) is inhibited and the affinity of an agonist (carbamylcholine) for the ACh receptor is enhanced. Prolonged exposure of ACh receptors to agonists induces a desensitized state that is characterized by a higher affinity for receptor agonists (31). Pyr increased the ability of carbamylcholine to inhibit [^{125}I]α-BGT binding to the receptor by 6-fold. This stimulation was only seen at concentrations at which Pyr inhibited [^{3}H]PCP and [^{3}H]H_{12}-HTX binding to the ion channel. Pyr appeared to have a higher affinity for receptor than for ion channel binding sites. Thus, Pyr acts as a typical receptor ligand in its influence on channel probe binding, stimulating [^{3}H]PCP and [^{3}H]H_{12}-HTX binding in the same concentration range as that at which it occupies receptor binding sites (i.e., inhibits [^{3}H]ACh binding). However, it should be noted that in terms of detection in binding studies the receptor and ion channel interactions of Pyr are antagonistic. That is, Pyr occupancy of receptor (i.e., ACh) binding sites enhances the binding of channel probes (e.g., [^{3}H]H_{12}-HTX and [^{3}H]PCP), thus obscuring any direct interactions of Pyr with the channel. These actions are distinct from AChE inhibition caused by the agent. When the action of the drug results in generation of nonconducting intermediates (see scheme below), the possibility exists that the binding of Pyr occurs at a site or sites that enhances the binding of ACh to the recognition site of the receptor (18, 26, 32–34). The following scheme may help to illustrate the formation of the nonconducting, or "desensitized," species *RI'*:

$$A_n + RI \underset{k_{-1}}{\overset{k_1}{\rightleftharpoons}} A_nRI \underset{k_{-2}}{\overset{k_2}{\rightleftharpoons}} A_nRI^*$$
$$\downarrow D \qquad\qquad \downarrow D$$
$$RI'D \rightleftharpoons A_nRI'D$$

where A_n represents the agonist; n represents the number of agonist molecules which are assumed to be 2; D represents the drug; and RI, RI^*, and RI' represent the receptor-ion channel complex in the "closed," "open" and "desensitized" (nonconducting) conformations, respectively. The drug (D) induces several rapidly equilibrating intermediates which have been limited here to the simplest case, two. The presence of such desensitized intermediates decreases the number of RI complexes

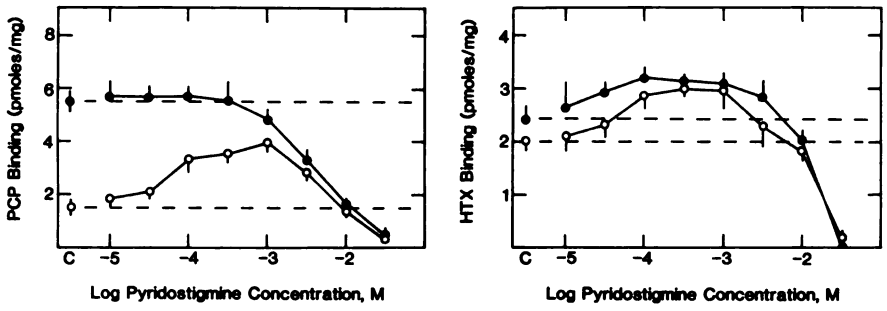

FIG. 11. *Influence of Pyr on the binding of probes to nicotinic synaptic ion channels in Torpedo electric organ*

The specific (i.e., amantadine-sensitive) binding of 3 nM [^{3}H]PCP (Fig. 3A) and 2 nM [^{3}H]H_{12}-HTX (Fig. 3B) was measured in the absence (○) and presence (●) of 1 μM carbamylcholine. Each point and line represents the mean and standard deviation from three determinations. *C* and the *dashed lines* indicate control binding measured in the absence of Pyr.

capable of being activated. This in turn would decrease responses which depend upon summation of ionic channel events, e.g., EPC amplitudes and ACh sensitivity.

Another mode of action of Pyr, i.e., a change in the conductance properties of the ion channel, is strongly indicated by the noise data (Tables 2 and 3; Fig. 7). In the presence of Pyr, γ was decreased while τ_I was apparently prolonged. The change in γ, a property of the open channel, cannot be due to either curarizing or desensitizing mechanisms. For several reasons, it is also most unlikely that AChE inhibition is involved in the channel property changes which we have observed. First, the effect of Pyr could be observed even after the tissue was exposed to 1 mM DFP (Table 3). Second, AChE blockade in itself will not alter γ or τ_I as measured by noise analysis (see Table 3, wash after DFP, and ref. 22). Two possibilities may account for the receptor-channel effects produced by Pyr. The binding of Pyr to the functional A_nRI complex may change the properties of the active channel, or the agent may generate ionic channels with low conductance as a weak agonist (Pyr + $R \rightleftharpoons$ PyrR^*) [see Akaike *et al.* (13)]. The scheme described above might be a reasonable corollary to the agonist and desensitizing effects at high concentrations. To test these hypotheses, an attempt was made to apply Pyr alone microiontophoretically in order to produce EPC fluctuations at end-plates of the frog cutaneous pectoris. During the microiontophoresis of Pyr we were able to discern very small EPC fluctuations, many-fold smaller than the usual ACh-induced fluctuations. The signal-to-noise ratio made the analysis of these recordings of the single elementary phenomenon in the junctional region rather difficult. The small transient currents may be due to channels that are activated by Pyr itself. Thus, strong evidence suggests that the direct influences of Pyr involve at least three distinct, although possibly interacting, mechanisms: (a) a weak agonist action, (b) the formation of desensitized intermediates, and (c) the alteration of the conductance properties of active channels.

In summary, the studies described above and the patch clamp studies of the following paper (13) demonstrate that Pyr has a direct effect on the ACh receptor ion channel complex.

ACKNOWLEDGMENTS

The authors are indebted to Ms. Mabel Zelle and Mrs. Laurie Aguayo for computer assistance, to Mrs. Barbara Marrow for technical assistance, and to Mrs. Margaret Shimkaveg for preparation of the typescript.

REFERENCES

1. Drachman, D. B. The biology of myasthenia gravia. *Annu. Rev. Neurosci.* **4**:195–225 (1981).
2. Dirnhuber, P., M. C. French, D. M. Green, L. Leadbeater, and J. A. Stratton. The protection of primates against soman poisoning by pretreatment with pyridostigmine. *J. Pharm. Pharmacol.* **31**:295–299 (1979).
3. Shaw, K. P., A. Akaike, and E. X. Albuquerque. The anticholinesterase agent, physostigmine (Phy), blocks the ionic channel of the nicotinic receptor in its open conformation. *Neurosci. Abstr.* **9**:1138 (1983).
4. Eccles, J. C., and W. V. MacFarland. Actions of anti-cholinesterases on endplate potential of frog muscle. *J. Neurophysiol.* **12**:59–80 (1949).
5. Katz, B., and R. Miledi. The nature of the prolonged endplate depolarization in anti-esterase treated muscle. *J. Physiol. (Lond.)***192**:27–38 (1975).
6. Magleby, K. L., and D. A. Terrar. Factors affecting the time course of decay of end-plate currents: a possible cooperative action of acetylcholine on receptors of the frog neuromuscular junction. *J. Physiol. (Lond.)* **244**:467–495 (1975).
7. Kuba, K., E. X. Albuquerque, J. Daly, and E. A. Barnard. A study of the irreversible cholinesterase inhibitor, diisopropylfluorophosphate, on time course of end-plate currents in frog sartorius muscle. *J. Pharmacol. Exp. Ther.* **189**:499–512 (1974).
8. Kordas, M., M. Brzin, and Z. Majcen. A comparison of the effect of cholinesterase inhibitors on end-plate current and on cholinesterase activity in frog muscle. *Neuropharmacology* **14**:791–800 (1975).
9. Riker, W. F., Jr., and F. G. Standaert. The action of facilitatory drugs and acetylcholine on neuromuscular transmission. *Ann. N. Y. Acad. Sci.* **135**:163–176 (1966).
10. Duncan, C. J., and S. J. Publicover. Inhibitory effects of cholinergic agents on the release of transmitter at the frog neuromuscular junction. *J. Physiol. (Lond.)* **294**:91–103 (1979).
11. Seifert, S. A., and M. E. Eldefrawi. Affinity of myasthenic drugs to acetylcholinesterase and acetylcholine receptor. *Biochem. Med.* **10**:258–265 (1974).
12. Carpenter, D. O., L. A. Greene, W. Shain, and Z. Vogel. Effects of eserine and neostigmine on the interaction of α-bungarotoxin with *Aplysia* acetylcholine receptors. *Mol. Pharmacol.* **12**:999–1006 (1976).
13. Akaike, A., S. R. Ikeda, N. Brookes, G. J. Pascuzzo, D. L. Rickett, and E. X. Albuquerque. The nature of the interactions of pyridostigmine with the nicotinic acetylcholine receptor-ionic channel complex. II. Patch clamp studies. *Mol. Pharmacol.* **25**:102–112 (1984).
14. Takeuchi, A., and N. Takeuchi. Active phase of frog's end-plate potential. *J. Neurophysiol.* **22**:395–411 (1959).
15. Masukawa, L. M., and E. X. Albuquerque. Voltage- and time-dependent action of histrionicotoxin on the endplate current of the frog muscle. *J. Gen. Physiol.* **72**:351–367 (1978).
16. Anderson, R., and C. F. Stevens. Voltage clamp analysis of acetylcholine produced end-plate current fluctuations at frog neuromuscular junction. *J. Physiol. (Lond.)* **235**:655–691 (1973).
17. Adler, M., A. C. Oliveira, E. X. Albuquerque, N. A. Mansour, and A. T. Eldefrawi. Reaction of tetraethylammonium with the open and closed conformations of the acetylcholine receptor ionic channel complex. *J. Gen. Physiol.* **74**:129–152 (1979).
18. Maleque, M. A., C. Souccar, J. B. Cohen, and E. X. Albuquerque. Meproadifen reaction with the ionic channel of the acetylcholine receptor: potentiation of agonist-induced desensitization of the frog neuromuscular junction. *Mol. Pharmacol.* **22**:636–647 (1982).
19. Aronstam, R. S., J. L. Graham, and L. Narayanan. Receptor-ion channel interactions in *Torpedo* electric organ: influence of thiol group modification. *Neurosci. Lett.* **31**:53–58 (1982).
20. Lowry, O. H., N. J. Rosebrough, A. L. Farr, and R. J. Randall. Protein measurement with the Folin phenol reagent. *J. Biol. Chem.* **193**:265–275 (1951).
21. Aronstam, R. S., A. T. Eldefrawi, I. N. Pessah, J. W. Daly, E. X. Albuquerque, and M. E. Eldefrawi. Regulation of [^{3}H]perhydrohistrionicotoxin binding to *Torpedo ocellata* electroplax by effectors of the acetylcholine receptors. *J. Biol. Chem.* **256**:2843–2850 (1981).
22. Carp, J. S., R. S. Aronstam, B. Witkop, and E. X. Albuquerque. Electrophysiological and biochemical studies on enhancement of desensitization by phenothiazine neuroleptics. *Proc. Natl. Acad. Sci. U. S. A.* **80**:310–314 (1983).
23. Mandell, J. D., and A. D. Hershey. A fractionating column of nucleic acids. *Anal. Biochem.* **1**:66–77 (1960).
24. Adler, M., E. X. Albuquerque, and F. J. Lebeda. Kinetic analysis of end plate currents altered by atropine and scopolamine. *Mol. Pharmacol.* **14**:514–529 (1978).
25. Tsai, M.-C., N. A. Mansour, A. T. Eldefrawi, M. E. Eldefrawi, and E. X. Albuquerque. Mechanism of action of amantadine on neuromuscular transmission. *Mol. Pharmacol.* **14**:787–803 (1978).
26. Feltz, A., and A. Trautmann. Desensitization at the frog neuromuscular junction: a biphasic process. *J. Physiol. (Lond.)* **322**:257–272 (1982).
27. Katz, B., and R. Miledi. The characteristics of 'end-plate noise' produced by different depolarizing drugs. *J. Physiol. (Lond.)* **230**:707–717 (1973).
28. Spivak, C. E., B. Witkop, and E. X. Albuquerque. Anatoxin-a: a novel, potent agonist at the nicotinic receptor. *Mol. Pharmacol.* **18**:384–394 (1980).
29. Gillies, J. D., and J. Allen. Effects of neostigmine and pyridostigmine at the neuromuscular junction. *Clin. Exp. Neurol.* **14**:271–279 (1977).
30. Alderdice, M. T. Further comparison of the effects of physostigmine and neostigmine on frog neuromuscular transmission. *Clin. Exp. Pharmacol. Physiol.* **9**:35–43 (1982).
31. Weber, M., T. David-Pfeuty, and J.-P. Changeux. Regulation of binding properties of the nicotinic receptor protein by cholinergic ligands in membrane from *Torpedo marmorata*. *Proc. Natl. Acad. Sci. U. S. A.* **72**:3443–3447 (1975).
32. Heidmann, T., and J.-P. Changeux. Fast kinetic studies on the interaction of a fluorescent agonist with the membrane-bound acetylcholine receptor from *Torpedo marmorata*. *Eur. J. Biochem.* **94**:255–279 (1979).
33. Feltz, A., and A. Trautmann. Interaction between nerve-released acetylcholine and bath applied agonists at the frog end-plate. *J. Physiol. (Lond.)* **322**:257–272 (1982).
34. Magleby, K. L., and B. S. Palotta. A study of desensitization of acetylcholine receptors using nerve-released transmitter in the frog. *J. Physiol. (Lond).* **316**:225–250 (1981).

Send reprint requests to: Dr. Edson X. Albuquerque, Department of Pharmacology and Experimental Therapeutics, University of Maryland School of Medicine, Baltimore, Md. 21201.